A new DNA nanostructure, the G-wire, imaged by scanning probe microscopy

Thomas C. Marsh, James Vesenka and Eric Henderson*

Department of Zoology and Genetics, 2112 Molecular Biology Building, Iowa State University, Ames, IA 50011, USA

ABSTRACT

G-DNA is a polymorphic family of quadruple helical nucleic acid structures containing guanine tetrad motifs [G-quartets; Williamson,J.R., Raghuraman,M.K. and Cech,T.R. (1989) *Cell* 59, 871–880; Williamson,J.R. (1993) *Proc. Natl. Acad. Sci. USA* 90, 3124–3124]. Guanine rich oligonucleotides that are self-complimentary, as found in many telomeric G-strand repeat sequences, form G-DNA in the presence of monovalent and/or divalent metal cations. In this report we use the atomic force microscope (AFM) to explore the structural characteristics of long, linear polymers formed by the telomeric oligonucleotide d(GGGG TTGGGG) in the presence of specific metal cations. In the AFM these polymers, termed G-wires, appear as filaments whose height and length are determined by the metal ions present during the self-assembly process. The highly ordered, controllable self-assembly of G-wires could provide a basis for developing advanced biomaterials.

INTRODUCTION

Formation of ordered structures by molecular self-assembly has been pursued as an effective strategy for development biomaterials for nanotechnology applications (3,4). The variety of conformations that nucleic acid sequences can adopt provide numerous opportunities to create useful nanostructures, primarily as scaffolds (5). Custom synthesis of oligonucleotides is reliable and relatively inexpensive. Moreover, the methods by which nucleic acids can be derivatized (6) provides a mechanism for construction of nanostructures with diverse chemical and physical characteristics. Cube-shaped, branched, knotted and other structures have been constructed using double helical DNA (7–9). Those structures are based upon Watson–Crick complimentarity and have the potential to form two- and three-dimensional arrays.

The ability of some nucleic acids to recognize not only their Watson–Crick compliment but also their twin enhances their potential to form useful nanostructures. G-DNA is a very stable four-stranded structure containing a planar, tetrameric arrangement of guanines termed the G-quartet (Fig. 3, inset) (1). Short G-rich oligonucleotides with at least three consecutive guanines

can form G-DNA structures in the presence of specific class Ia (Na^+, K^+, Rb^+) and IIa (Mg^{2+}, Ca^{2+}, Ba^{2+}, Sr^{2+}) metal cations (10). Formation of G-DNA superstructures limited to four or five repeats has been demonstrated for 3' end self-complimentary G4-DNA (a subclass of G-DNA; Fig. 3d) (11,12). We have utilized G4-DNA as a system for creating large, self-assembling nanostructures using the simple 10 nucleotide sequence, d(GGGGTTGGGG) ($Tet_{1.5}$), that is self-complementary at its 5' and 3' ends (13). We call these structures G-wires (Fig. 3).

Numerous studies have proven the utility of the AFM (14) as a powerful tool for imaging and analyzing nucleic acids (15–18). In the AFM, interactions between a sharp stylus and the sample are detected as the tip scans the sample. The tip may be in constant or transient contact with the sample and the force applied precisely controlled. The data collected can be displayed as a 3-D topograph of the sample, with sub-Angstrom accuracy in the Z (height) dimension. Here, the AFM is used for the first time to make direct measurements of a new DNA structure, the G-wire.

MATERIALS AND METHODS

Preparation of oligonucleotide

Oligonucleotides were synthesized using standard phosphoramidite chemistry. Purification of the oligonucleotide was performed by denaturing gel electrophoresis as previously described (19). Lyophilized oligonucleotide was dissolved in 80% formamide, 53 mM Tris–HCl, 53 mM Boric acid, 0.9 mM EDTA (0.6 × TBE, final pH 8.3) loading buffer and denatured in a boiling water bath for 5 min. The oligonucleotide was loaded on a 30 cm long 1.5 mm thick 20% polyacrylamide, 0.6 × TBE gel and separated by electrophoresis at 800 V. The electrophoresis was stopped when the bromophenol blue tracking dye in a separate lane reached 5 cm from the gel bottom. The oligonucleotide was visualized by UV shadowing, cut from the gel and eluted overnight in 10 mM Tris–HCl (pH 8.0), 1 mM EDTA (TE). The oligonucleotide was concentrated and desalted by C18 (Waters) column chromatography. 2.5 µg aliquots of $Tet_{1.5}$ were diluted in water and denatured by boiling followed by rapid cooling and lyophilization.

Atomic force microscopy (AFM)

$Tet_{1.5}$ was dissolved in the appropriate buffer and incubated at 37°C for 12–24 h. After incubation the samples were diluted

---

* To whom correspondence should be addressed

1:100 in 10 mM Tris–HCl, pH 7.5, 1 mM MgCl$_2$ and 10 µl was deposited onto a freshly cleaved mica substrate. The G-wires were allowed to adsorb for 5 min, washed with 1 ml sterile water, and rapidly dried in a stream of N$_2$ gas. Imaging was performed with 125 µm Si tapping probes at relative humidity ≤10% using a Nanoscope III equipped with a D-scanner (Digital Instruments, Inc.).

Gel electrophoresis

Tet$_{1.5}$ was radiolabeled internally with ^{32}P as described previously (13). The extent of G-wire formation in 50 mM NaCl, 5 mM KCl, 10 mM MgCl$_2$; 50 mM NaCl, 10 mM MgCl$_2$; 50 mM KCl, 10 mM MgCl$_2$ and TE, pH 7.5 was determined by electrophoresis on native and denaturing polyacrylamide gels. Salt solutions were buffered with 50 mM Tris–HCl, pH 7.5. All samples were incubated 24 h at 37°C and then separated by electrophoresis through a 15% acrylamide, 0.6 × TBE gel (native) or a 15% acrylamide, 0.6 × TBE, 8 M urea gel (denaturing). Loading buffer for native electrophoresis contained 20% sucrose, 1.2 × TBE, while loading buffer for denaturing electrophoresis contained 80% formamide, 1.2 × TBE, 0.05% bromophenol blue and 0.05% xylene cyanole FF. Each G-wire solution was mixed 1:1 with loading buffer and applied to the gels without boiling.

RESULTS

G-wires self-assemble into long filamentous polymers

The self-assembly of G-wires was found to occur efficiently at 37°C in buffer containing 50 mM NaCl, 10 mM MgCl$_2$, 1 µM spermidine and 50 mM Tris–HCl pH 7.5 (Na$^+$/Mg^{2+}/spermidine) (13). G-wires grown in Na$^+$/Mg^{2+}/spermidine buffer were examined by AFM which revealed that they were polydisperse linear polymers (Fig. 1). The length of G-wires ranged from 10 to > 1000 nm. The height and width of the G-wires was found to be uniform with few bends, kinks or branches. This indicated that G-wires were ordered, relatively rigid polymers. The height of G-wires was found to be two to three times greater than the height plasmid DNA in the AFM (Fig. 1, g–i and Table 1).

Table 1. Height comparison of G-wires and plasmid DNA

G-wire growth conditions	Measured height (Å)	
Na$^+$/Mg^{2+}	16.9 ± 1.4	$n = 90$
K$^+$/Mg^{2+}	23.1 ± 2.0	$n = 100$
Mg^{2+}	12.7 ± 1.6	$n = 50$
Na$^+$/Mg^{2+}/spermidine	23.9 ± 1.1	$n = 150$
Plasmid (pSK II)	6.3 ± 1.1	$n = 161$

Measurements of the heights of G-wires grown in the listed buffers encompass data from at least two different sample preparations. The number of individual data points/sample used to calculate averages is indicated (n).

Magnesium induced synergy of G-wire self-assembly

In the AFM G-wires appeared as relatively straight, variable length polymers, as expected for a tubular structure with a central canal filled with a tight fitting cation. The length of G-wires is a function of the incubation conditions with particular dependence upon ionic environment, temperature and time. This dependence
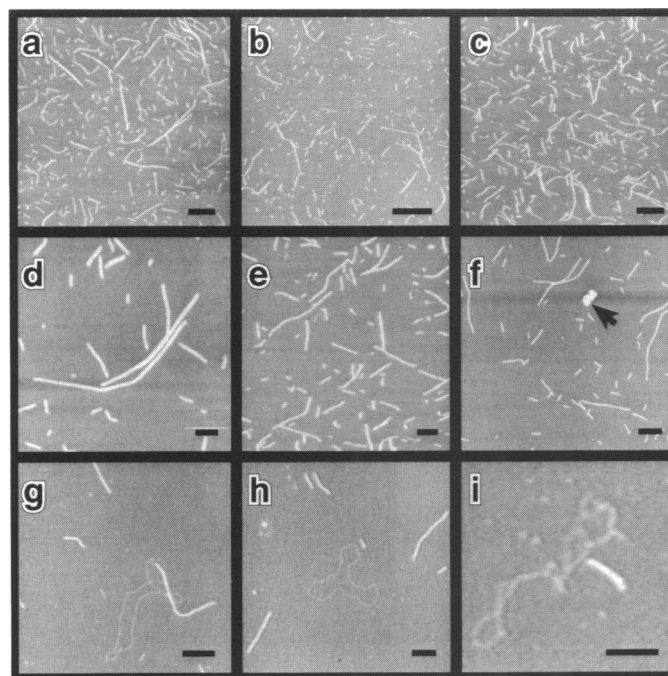

Figure 1. AFM gallery of G-wires grown in the presence of spermidine. The average height of the G-wires is 23.9 ± 1.1 Å and the lengths range from 10 to >1000 nm. (a–i) are G-wires grown with Tet$_{1.5}$ at a concentration of 0.25 µg/µl in buffer containing 50 mM NaCl, 50 mM Tris–HCl, pH 7.5, 10 mM MgCl$_2$ and 1 µM spermidine at 37°C for 12–24 h. Panel f is an image of G-wires deposited with 15 nm colloidal gold (indicated by arrow) as an internal height standard. Panels g–i are G-wires deposited with pSKII (Stratagene) plasmid DNA. The apparent height of the plasmid DNA was ~7 Å. Images were collected with a Nanoscope III D-scanner (Digital Instruments, Inc.) using contact and tapping modes (32). Scale bars: a and b = 500 nm, c = 200 nm, d = 50 nm, e–i = 100 nm.

is shown by AFM imaging (Fig. 2a) and gel electrophoresis (Fig. 2b) of G-wires grown under various conditions. In Na$^+$ or K$^+$ alone, relatively short G-wires were generated. In Mg^{2+}, longer G-wires were observed at low frequency. The longest and most plentiful G-wires were grown in Na$^+$/Mg^{2+} buffer. K$^+$/Mg^{2+} grown G-wires were somewhat shorter in length than Na$^+$/Mg^{2+} G-wires and more structurally heterogeneous. The corresponding gel electrophoresis of G-wire incubations reflected these results. Denaturing gels contained 8 M urea and were used in some cases to remove less stable structural species that result in a background smear on non-denaturing gels (see Materials and Methods).

AFM height measurements and G-wire stability

The heights of G-wires depended upon the growth conditions. These data are summarized in Table 1. K$^+$/Mg^{2+} grown G-wires had an average height of 23.1 ± 2.0 Å. G-wires grown in Na$^+$/Mg^{2+} buffer have an average height of 16.9 ± 1.4 Å. Those formed in Mg^{2+} alone had an average height of 12.7 ± 1.6 Å. This difference in heights suggests that G-wire compressibility is a function of cationic growth conditions. Additional buttressing of the structure may be conferred by cation (e.g., Mg^{2+}) binding to the external surface. Although spermidine was not required for G-wire formation (Fig. 2a and b), a significant increase in G-wire height was observed when spermidine was present in the growth buffer (Table 1). The gallery of G-wires grown in Na$^+$/Mg^{2+}/spermidine buffer is shown in Figure 1. Spermidine and spermine
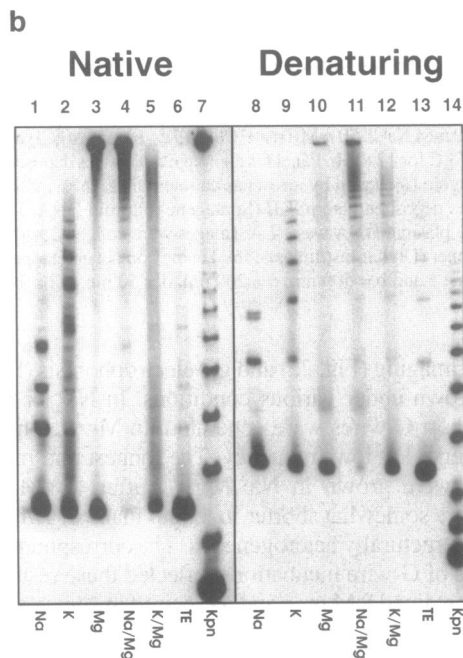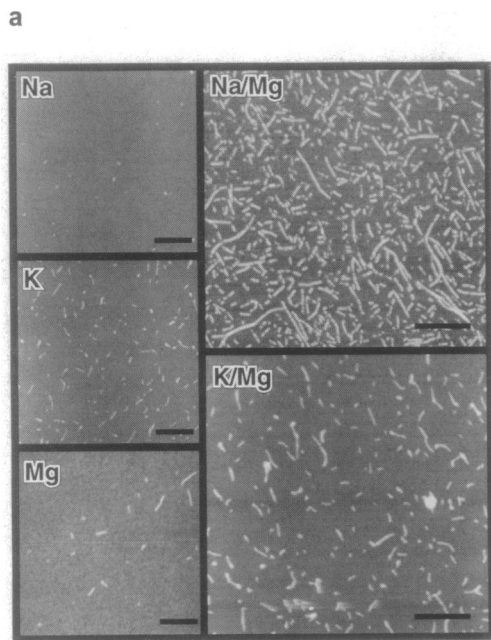
a

b

Figure 2. Tapping mode (32) AFM images and electrophoretic analysis of Tet$_{1.5}$ G-wires grown in different buffer conditions. Conditions used for G-wire growth were identical for AFM and gel analyses. (a) After incubation the samples were diluted 1:100 in 10 mM Tris–HCl, pH 7.5, 1 mM MgCl$_2$ and deposited onto a freshly cleaved mica substrate. The samples were incubated for 5 min, washed with 1 ml sterile water and rapidly dried in a stream of N$_2$ gas. Imaging was performed with 125 µm Si tapping probes at relative humidity =10% using a Nanoscope III with a D-scanner (Digital Instruments, Inc.). The scale bar = 250 nm. (b) Native and denaturing gels show the extent of G-wire formation in 50 mM NaCl, 5 mM KCl, 10 mM MgCl$_2$; 50 mM NaCl, 10 mM MgCl$_2$; 50 mM KCl, 10 mM MgCl$_2$ and TE, lanes 1–6 respectively. Lane 7 contains 8 bp *Kpn*I linker oligonucleotide ligation ladder. Samples were incubated for 24 h at 37°C and then analyzed on 15% acrylamide, 0.6 × TBE gels (denaturing gels included 8 M urea).

are known to bind to double helical regions of tRNA (20) and duplex DNA (21). Triple helical DNA formation is also enhanced by the presence of such polycations (22). The apparent increase
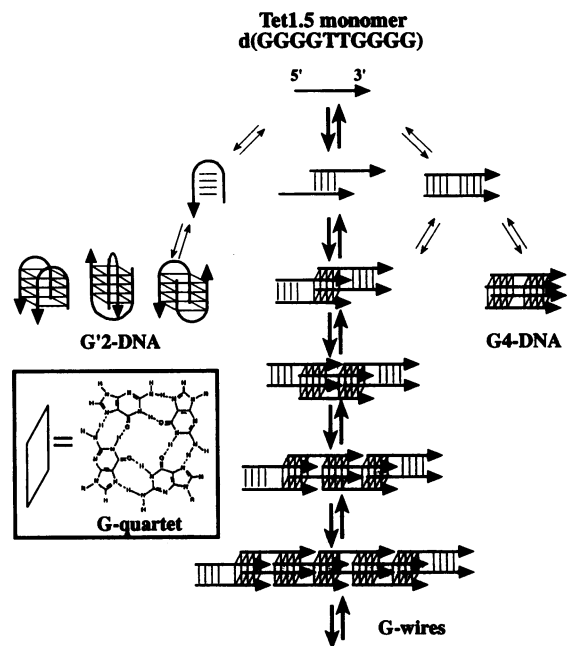

Figure 3. Comparison of G-DNA conformations that Tet$_{1.5}$ may adopt. The central path of structure formation involves the formation of an out-of-register G4-DNA conformation that is initially less favored than the other competing conformations. The potential for continually increasing the stability of G-wires, by means of bidirectional G4-DNA formation, ultimately favors G-wire formation. The equilibrium between competing structures is modulated by temperature, ionic species, concentration and 5′ stereochemistry of Tet$_{1.5}$.

in G-wire height in the presence of spermidine could be indicative of a true increase in molecular diameter due to spermidine binding or improved resistance to compression forces from the scanning probe.

Model of G-wire assembly

The alternative pathways of structure formation for Tet$_{1.5}$ are depicted in Figure 3. The oligonucleotide d(GGGGTTGGGG) has been reported to form hairpin dimer (G′2-DNA) and parallel tetramer (G4-DNA) G-DNA conformations (23). In addition to these structures, we showed previously that this molecule can spontaneously self-assemble into polymers called G-wires (13). The concentration of DNA, cationic environment and the presence of a 5′ phosphate group on Tet$_{1.5}$ dictate what conformations predominate.

DISCUSSION

The height of G-wires measured in the AFM under some conditions was close to the diameter of G-quartets determined by X-ray crystallography (~28 Å) (24,25). In contrast, B-form DNA appears much flatter in the AFM than predicted from its molecular diameter of ~20 Å, with observed heights typically in the range of 5–10 Å (Fig. 1g, h and i) (17,26,27). The reduced height of B-DNA is probably caused by a number of factors which include sample compression (28) and/or friction related artifacts (29). Friction artifacts can be revealed and compensated for by examination of apparent heights in both scan directions (30) and did not play a role in the observed height of G-wires (data not shown). Thus, G-DNA appears to be more resistant to
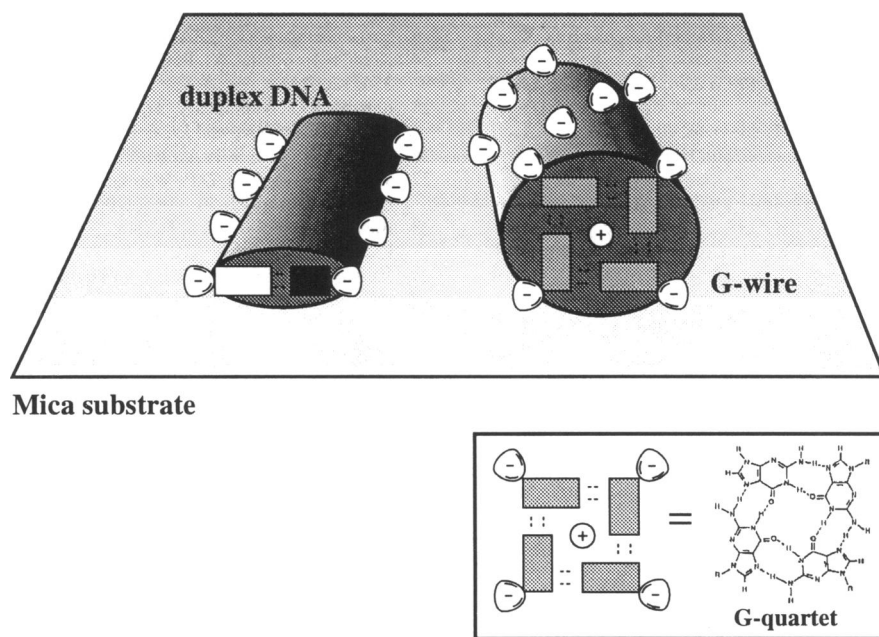
Figure 4. Model of differential stability of duplex DNA and tetraplex DNA during imaging by AFM. The height of plasmid DNA is significantly diminished compared to the height of the G-wire. A possible explanation is that an uncoiling of the double helix occurs as the DNA molecule is adsorbed to the substrate and dried (31). The quadruple helical G-wires have a coordinated cation that provides additional stability to the structure, thereby providing resistance to conformation change upon surface binding. The heights of the G-wires correlate with the stabilizing capacity of the coordinated cation ($K^+ > Na^+ > Mg^{2+}$) (10).

compression in the AFM than does B-DNA. The reduced compressibility of G-wires implies that structures based on the G-quartet motif are structurally robust, which is not unexpected for an ion filled tube. An alternative explanation for reduced height of B-DNA imaged by AFM is relaxation of the helix such that it lies flat on the substrate in a non-helical 'railroad track' configuration (31), which might facilitate sequence determination by scanning probe methods. Nicked circle and linear B-DNA could topologically accommodate unwinding of the helix if surface binding forces were sufficient to induce this degree of distortion. In this case, a quadruple helical structure would have greater resistance to this type of conformation change and, therefore, appear taller. This idea is illustrated in Figure 4.

Formation of G-wire polymers depends upon G-quartets as a basis of self-complimentarity and stability. The ability of Tet$_{1.5}$ to self-assemble into long polymers clearly demonstrates its potential as scaffold structures for nanotechnology applications. G-wires are structurally more robust than duplex DNA when imaged by AFM. This feature is important when considering manipulation of structures by the scanning tip. Nucleic acids can be readily chemically modified with functional moieties, which vastly increases their potential as scaffolds for nanostructure design and construction. Synthesis of branched oligonucleotides would also facilitate self-assembly of 2-D and possibly 3-D networks. Thus, formation of nucleic acid nanostructures utilizing guanine self-recognition would be comparable to the DNA cubes and knots constructed using duplex DNA. In addition to a scaffold role, some of the physical properties of G-wires, such as the central canal within which cations reside and an electron-rich external surface, suggest that they may be useful as functional components of nanoscale electronic devices. Moreover, it may be possible to exploit ion dependent structural variation in G-wires in the construction of novel ion biosensors.

ACKNOWLEDGEMENTS

REFERENCES

1 Williamson, J.R., Raghuraman, M.K. and Cech, T.R. (1989) *Cell* **59**, 871–880.
2 Williamson, J.R. (1993) *Proc. Natl. Acad. Sci. USA* **90**, 3124–3124.
3 Whitesides, G.M., Mathias, J.P. and Seto, C.T. (1991) *Science* **254**, 1312–1318.
4 Ghadiri, M.R., Granja, J.R., Milligan, R.A., McRee, D.E. and Khazanovich, N. (1993) *Nature* **366**, 324–327.
5 Amato, I. (1993) *Science* **260**, 753–755.
6 Letsinger, R.L., Chaturvedi, S.K. and Farooqui, F. (1993) *J. Am. Chem. Soc.* **115**, 7535–7536.
7 Chen, J.H. and Seeman, N.C. (1991) *Nature* **350**, 631–633.
8 Du, S.M. and Seeman, N.C. (1994) *Biopolymers* **34**, 31–37.
9 Seeman, N.C. (1991) *DNA Cell Biol.* **10**, 475–86.
10 Venczel, E.A. and Sen, D. (1993) *Biochemistry* **32**, 6220–6228.
11 Sen, D. and Gilbert, W. (1992) *Biochemistry* **31**, 65–70.
12 Lu, M., Guo, Q. and Kallenbach, N.R. (1992) *Biochemistry* **31**, 2455–2459.
13 Marsh, T.C. and Henderson, E. (1994) *Biochemistry* **33**, 10718–10724.
14 Binnig, G., Quate, C.F. and Gerber, C. (1986) *Phys. Rev. Lett.* **56**, 930–933.

15 Allen, M.J., Fan Dong, X., O'Neill, T.E., Yau, P., Kowalczykowski, S.C., Gatewood, J., Balhorn, R. and Bradbury, E.M. (1993) *Biochemistry* **32**, 8390–8396.

16 Bustamante, C., Keller, D. and Yang, G. (1993) *Curr. Opin. Struct. Biol.* **3**, 363–372.

17 Hansma, H., Vesenka, J., Siegerist, C., Kelderman, G., Morret, H., Sinsheimer, R.L., Elings, V., Bustamante, C. and Hansma, P.K. (1992) *Science* **256**, 1180–1184.

18 Hansma, H.G., Bezanilla, M., Zenhausern, F., Adrian, M. and Sinsheimer, R.L. (1993) *Nucleic Acids Res.* **21**, 505–512.

19 Henderson, E., Hardin, C.C., Walk, S.K., Tinoco, I.J. and Blackburn, E.H. (1987) *Cell* **51**, 899–908.

20 Teeter, M.M., Quigly, G.J. and Rich, A. (1980) In Spiro, T.G. (ed.), *Nucleic Acid–Metal Ion Interactions*. John Wiley & Sons, Inc., New York, pp. 145–177.

21 Schmid, N. and Behr, J.-P. (1991) *Biochemistry* **30**, 4358–4361.

22 Hampel, K.J., Crosson, P. and Lee, J.S. (1991) *Biochemistry* **30**, 4455–4459.

23 Balagurumoorthy, P., Brahmachari, S.K., Mohanty, D., Bansal, M. and Sasisekharan, V. (1992) *Nucleic Acids Res.* **20**, 4061–4067.

24 Kang, C.H., Zhang, X., Ratliff, R., Moyzis, R. and Rich, A. (1992) *Nature* **356**, 126–131.

25 Laughlan, G., Murchie, A.I.H., Norman, D.G., Moore, M.H., Moody, P.C.E., Lilley, D.M. and Luisi, B. (1994) *Science* **265**, 520–524.

26 Bustamante, C. (1991) *Annu. Rev. Biophys. Chem.* **20**, 415–446.

27 Thundat, T., Allison, D.P., Warmack, R.J. and Ferrell, T.L. (1992) *Ultramicroscopy* **42–44**, 1101–1106.

28 Bustamante, C., Vesenka, J., Tang, C.L., Rees, W., Guthold, M. and Keller, R. (1992) *Biochemistry* **31**, 22–26.

29 Yang, J. and Shao, Z. (1993) *Ultramicroscopy* **50**, 157–170.

30 Vesenka, J., Manne, S., Gibberson, R., Marsh, T. and Henderson, E. (1993) *Biophys. J.* **65**, 992–997.

31 Yagil, G. and Sussman, J.L. (1986) *EMBO J.* **5**, 1719–1725.

32 Zhong, Q., Inniss, D., Kjoller, K. and Elings, V.B. (1993) *Surf. Sci. Lett.* **290**, 688–692.